Materials Science & Engineering C 103 (2019) 109766

Contents lists available at ScienceDirect

Materials Science & Engineering C

journal homepage: www.elsevier.com/locate/msec

Preparation and in vitro evaluation of radiolabeled HA-PLGA nanoparticles as novel MTX delivery system for local treatment of rheumatoid arthritis

R. Maydelid Trujillo-Nolasco[a,b], Enrique Morales-Avila[a,*], Blanca E. Ocampo-García[b], Guillermina Ferro-Flores[b], Brenda V. Gibbens-Bandala[a,b], Alondra Escudero-Castellanos[b,c], Keila Isaac-Olive[c]

[a] Universidad Autónoma del Estado de México, Facultad de Química Toluca-México, Mexico
[b] Instituto Nacional de Investigaciones Nucleares, Departamento de Materiales Radiactivos Ocoyoacac-México, Mexico
[c] Universidad Autónoma del Estado de México, Facultad de Medicina Toluca-México, Mexico

ARTICLE INFO

Keywords:
Radiosynovectomy
Smart drug delivery system
Lutetium-177
Methotrexate
Polymeric nanoparticles
Targeted therapy

ABSTRACT

Radiosynovectomy is a technique used to decrease inflammation of the synovial tissue by intraarticular injection of a β-emitting radionuclide, such as ^{177}Lu, which is suitable for radiotherapy due to its decay characteristics. Drug-encapsulating nanoparticles based on poly lactic-*co*-glycolic acid (PLGA) polymer are a suitable option to treat several arthritic diseases, used as anti-inflammatory drugs transporters of such as methotrexate (MTX), which has been widely used in the arthritis treatment (RA), and hyaluronic acid (HA), which specifically binds the CD44 and hyaluronan receptors overexpressed on the inflamed synovial tissue cells. The 1,4,7,10-Tetraazacyclododecane-1,4,7,10-tetraacetic acid (DOTA) was used as complexing agent of Lutetium-177 for radiotherapy porpoises. The aim of this research was to synthesize ^{177}Lu-DOTA-HA-PLGA(MTX) as a novel, smart drug delivery system with target-specific recognition, potentially useful in radiosynovectomy for local treatment of rheumatoid arthritis. The polymeric nanoparticle system was prepared and chemically characterized. The MTX encapsulation and radiolabelling were performed with suitable characteristics for its in vitro evaluation. The HA-PLGA(MTX) nanoparticle mean diameter was 167.6 nm ± 57.4 with a monomodal and narrow distribution. Spectroscopic techniques demonstrated the effective conjugation of HA and chelating agent DOTA to the polymeric nanosystem. The MTX encapsulation was 95.2% and the loading efficiency was 6%. The radiochemical purity was 96 ± 2%, determined by ITLC. Conclusion: ^{177}Lu-DOTA-HA-PLGA(MTX) was prepared as a biocompatible polymeric PLGA nanoparticle conjugated to HA for specific targeting. The therapeutic nanosystem is based on bi-modal mechanisms using MTX as a disease-modifying antirheumatic drug (DMARD) and ^{177}Lu as a radiotherapeutic component. The ^{177}Lu-DOTA-HA-PLGA(MTX) nanoparticles showed properties suitable for radiosynovectomy and further specific targeted anti-rheumatic therapy.

1. Introduction

Conventional treatment of rheumatic diseases is usually based on low doses of methotrexate (MTX), a disease-modifying anti-rheumatic drug (DMARD). The clinical management is commonly accompanied by systemic side effects such as suppression of the immune system, with an elevated risk of viral and bacterial infection. The common adverse effects of MTX are nausea, vomiting, anaemia, neutropenia, pulmonary fibrosis, diarrhoea, dermatitis, bone marrow depression, mucositis, bruising and hepatitis [19,33]. MTX acts as an anti-proliferative molecule (through inhibition of dihydrofolate reductase enzyme, DHFR) and an anti-inflammatory agent (by means of adenosine overproduction). It is widely reported that it has poor pharmacokinetics and has a narrow safety margin, which limits the therapeutic outcomes [1,20].

The target-specific delivery of traditional chemotherapeutic agents to a diseased area has made new approaches imperative, in order to minimize or even avoid introducing the cargo into critical normal tissues. Despite the advances in nanomedicine, the complexity implicated in predicting biological behaviour limits their clinical applications. Many approaches have been used to improve the pharmacological and therapeutic effects [12,21]. Several nanomaterials have been proposed

* Corresponding author at: Facultad de Química, Universidad Autónoma del Estado de México, Paseo Tollocan esq Paseo Colón S/N, Toluca, Estado de México C.P. 50120, Mexico.
E-mail address: emoralesav@uaemex.mx (E. Morales-Avila).

https://doi.org/10.1016/j.msec.2019.109766
Received 6 June 2018; Received in revised form 9 January 2019; Accepted 16 May 2019
Available online 19 May 2019
0928-4931/

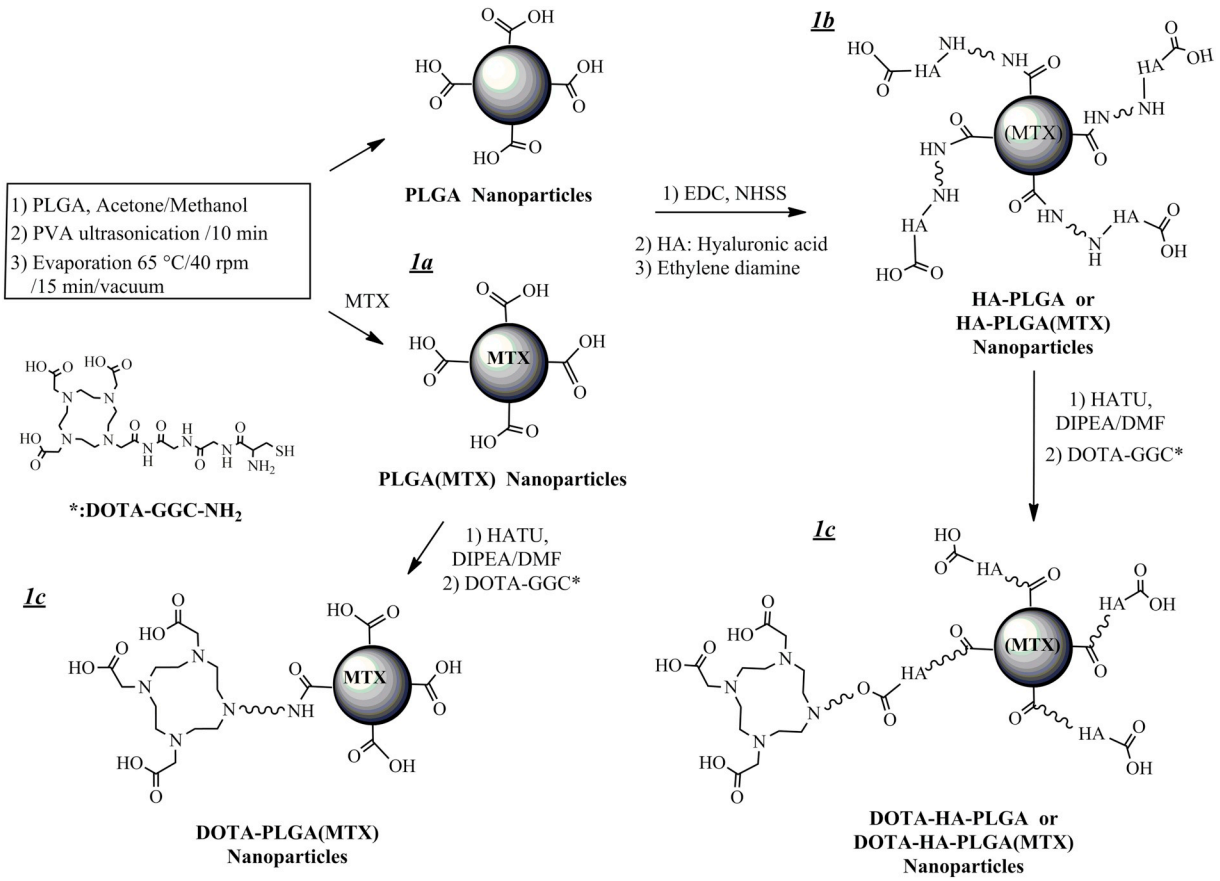

Fig. 1. Schematic synthesis of a) PLGA(MTX) nanoparticles, b) HA-PLGA or HA-PLGA(MTX) nanoparticles, c) DOTA-PLGA(MTX) and d) DOTA-HA-PLGA(MTX) nanoparticles.

as delivery systems to treat cancer or metabolic, chronic and degenerative diseases including osteoarticular disorders or rheumatic diseases. The inflamed synovial tissues contain activated macrophages, among other cells, which contribute to inflammation and joint destruction [31].

Hyaluronic acid (HA) specifically binds to cluster determinant 44 (CD44), a receptor that mediates various physiological and pathological processes. In pathogenic conditions, the CD44 receptor facilitates migration of damaged cells to vital organs, resulting in tissue and organ injury [26,29]. In patients suffering from Rheumatoid arthritis (RA), the inflamed synovial tissue contains activated macrophages, which overexpress CD44. The over-expression of CD44 is associated with the extent of inflammation [31].

Some studies regarding HA bound to the surface of nanoparticles have demonstrated that the nanoparticles (NPs) can effectively be accumulated in inflamed synovial tissues in RA animal models through the CD44 receptor [1].

Radiolabeled polymeric nanoparticles conjugated to biological molecules have demonstrated themselves capable of recognizing specific target sites; therefore, they can be a potential strategy to enhance therapeutic response rates and disease-free survival times. Lutetium-177 (^{177}Lu, half-life of 6.71 d) is a theragnostic radionuclide which enables radiotherapy due to its β max emission energy of 0.497 MeV (78%) and diagnosis through its γ radiation of 0.208 MeV (11%). It has been successfully used for targeted radiotherapy with efficient cross-fire effect in cancer cells [11,38]. Several antiarthritic radiopharmaceuticals have been proposed to treat joints in advanced stages of arthritis [40].

In this research, a new approach was designed, prepared, characterized and evaluated for producing dual therapy on macrophage cells over-expressing the CD44 receptor through MTX delivery as a disease-modifying antirheumatic drug and ^{177}Lu as the radiotherapeutic component. ^{177}Lu-DOTA-HA-PLGA(MTX) is proposed as a target-specific nanosystem with properties suitable for radiosynovectomy and for MTX therapy in RA.

2. Materials and methods

2.1. Materials

Poly(D,L-lactide-*co*-glycolide) acid terminated (PLGA; 50:50 lactide to glycolide ratio; MW: 40,300 g/mol), Poly(vinyl alcohol) (PVA, Mowiol® 4–88; MW: 31,000 g/mol), hyaluronic acid sodium salt from Streptococcus equi (MW: ~1.5–1.8 × 10^6 Da), N-(3-dimethylaminopropyl)-N′-ethylcarbodiimide hydrochloride (EDC), N-hydroxysulfosuccinimide sodium salt (NHSS), methotrexate (MTX) (MW: 454.4 g/mol), HATU (O-(7-azabenzotriazol-1-yl)-1,1,3,3-tetramethyl uroniumhexafluoro phosphate), XTT Kit II and other chemical reagents were purchased from Sigma-Aldrich (St. Louis, MO, USA) and used as received.

The DOTA-GGC (1,4,7,10-tetraazacyclododecane-N′,N″,N‴-tetraacetic-Gly-Gly-Cys) was synthesized and characterized by piChem (Graz, Austria) as previously described [38]. $^{177}LuCl_3$ was obtained from ITM Isotope Technologies Garching München AG (Garching, Germany). The RAW 264.7 cell line (murine macrophage) was obtained from ATCC (Atlanta, GA, USA).

2.2. Methods

2.2.1. Preparation of PLGA nanoparticles

PLGA nanoparticles were prepared by the single emulsification-solvent evaporation method [17,34]. Some modifications to the procedure were performed. Briefly, 1 mL of PLGA/acetone solution

(15 mg/mL) was added to 1.32 mL of methanol and stirred via vortex for 15 s. The solution was then slowly dropped over a solution of PVA (7.3 mL, 0.25% w/v) and the mixture was sonicated for 10 min in an ice bath. Acetone and methanol were eliminated by vacuum with a rotary evaporator (67 °C, 40 rpm, 20 min). Nanoparticles were purified by centrifugal filtration dialysis (MWCO 30 kDa; 4400 rpm for 30 min). The filtrate was suspended, lyophilized and stored for physicochemical characterization (DLS, SEM, FT-IR) and further use.

2.2.2. Preparation of the PLGA(MTX) nanoparticles

PLGA(MTX) nanoparticles (Fig. 1a) were prepared with the nanoparticles described above. In order to optimize the drug loading capacity in the nanoparticle systems, increased concentrations of MTX (100 to 1000 μg/mL) were added to the mixture. After the reaction time, the nanoparticle suspension was recovered via a centrifugal filtration dialysis system (MWCO 30 kDa; centrifugation of 4400 rpm for 30 min). The amount of encapsulated drug was determined indirectly by measuring free MTX in the supernatant (UV–Vis; $\lambda = 304$ nm) in relation to the initial amount added. The encapsulation efficiency (% EE) and loading efficiency (% LE) were calculated using an indirect method, where MTX_{added} is the amount (100 to 1000 μg/mL) added to the mixture, and MTX_{free} is the amount not encapsulated.

$$\%EE = \frac{MTX_{added} - MTX_{free}}{MTX_{added}} \times 100$$

$$\%\mathrm{LE} = \frac{MTX_{added} - MTX_{free}}{PLGA_{added}} \times 100$$

2.2.3. Hyaluronic Acid (HA) conjugation to PLGA and PLGA(MTX) nanoparticles

A hyaluronic acid solution (pH 4.75; 1 mL; 1.25 mM) was added to 9 mL of PLGA or PLGA(MTX) nanoparticles (0.01 g) in injectable-grade water, along with 0.0479 g of EDC (25 mM) and 0.0108 g of NHSS (5 mM). This solution was stirred for 4 h at room temperature. Then, 1 mL of EDA solution (0.003 g) in water was added to the HA solution and the mixture was stirred for 4 h at room temperature to obtain HA-PLGA and HA-PLGA(MTX) conjugated nanoparticles. The mixture was purified via a centrifugal filtration dialysis system (MWCO 30 kDa). Finally, HA-PLGA and HA-PLGA(MTX) nanoparticles were washed and suspended in 2 mL of injectable-grade water (Fig. 1b).

2.2.4. DOTA conjugation to PLGA(MTX), HA-PLGA or HA-PLGA(MTX) nanoparticles

Lyophilized PLGA(MTX) (4 mg), HA-PLGA (2.4 mg) or HA-PLGA(MTX) (1.1 mg, equivalent to 2.3×10^{-4} mmol of MTX) nanoparticles were dissolved in 40 μL of injectable-grade water and 100 μL of DMF. Afterwards, 8.1, 4.8 and 2.2 mg of HATU were respectively added (2:1 wt/wt, with regard to NPs), as a carboxylic acid-activator, to a 100 μL of DMF, followed by the addition of 100 μL of DIPEA (10 μL DIPEA/300 μL DMF). The mixture was stirred for 15 min at room temperature. Then, 100 μL of DOTA (1 mg/100 μL DMF) was added and the mixture was stirred for 1 h at room temperature. Finally, the mixture was purified through dialysis (MWCO 30 KDa) (Fig. 1c and d).

2.2.5. Preparation of radiolabelled nanoparticles with ^{177}Lu

Briefly, a 100 μL aliquot of DOTA-PLGA, DOTA-HA-PLGA and DOTA-HA-PLGA(MTX) (1 mg/250 μL sterile H_2O) was diluted with 100 μL of 1 M acetate buffer at pH 7.0, followed by the addition of 10 μL (3 MBq) of the $^{177}LuCl_3$ solution (ITG, Germany). The mixture was incubated at 37 °C in a dry block heater for 3 h. The solution was then centrifuged at 2500 *g* for 20 min (MWCO 30 KDa). The ^{177}Lu-DOTA-HA-PLGA and ^{177}Lu-DOTA-HA-PLGA(MTX) nanoparticles were washed twice with 2 mL of sterile water. The membrane activity, corresponding to ^{177}Lu-DOTA-HA-PLGA, ^{177}Lu-DOTA-HA-PLGA(MTX) and free ^{177}Lu in the filtered solution, was measured in a dose calibrator (Capintec, USA). In order to calculate the radiochemical purity, ITLC with a mobile phase of NaCl 0.9% and HCl 0.02 M, was performed, where free lutetium was identified at the solvent front.

2.3. Chemical characterization

2.3.1. Nanoparticle size and zeta potential

Particle size and Z potential were measured by dynamic light scattering (DLS), using a Nanotrac analyzer (Nanotrac Wave, Model MN401, Microtract, FL, USA). The analyses were performed with a wavelength of 657 nm at 20 °C, current of 15.79 mA, electric field of 14.35 V/cm and a sampling time of 128 μs, in aqueous solution. For each sample, the mean diameter, standard deviation and polydispersity index (PDI) were reported. Zeta potential was measured in diluted samples to assure an adequate and constant ionic strength. Each sample was measured in triplicate.

2.3.2. Scanning Electron Microscopy (SEM)

Size, shape and topography were evaluated with a JEOL JSM 6510LV microscope operating at 20 kV, using secondary electron signals. Samples were sputtered with a gold thin layer of approximately 15 nm using a Denton Vacuum DESK IV system.

2.3.3. FT-IR spectroscopy

The IR spectra of raw materials and lyophilized samples were acquired using a PerkinElmer System 2000 spectrometer with an ATR platform (Pike Technologies), by applying attenuated total reflection Fourier transform infrared (ATR-FT-IR) spectroscopy. The spectra were acquired with 40 scans, in an operating range of 4000–400 cm^{-1} and a resolution of 0.4 cm^{-1}.

2.3.4. UV–Vis spectroscopy

Nanoparticle suspensions were measured through UV–Vis analysis in order to monitor the conjugation reactions. Analysis were carried out in a Thermo Genesys 10S UV–Vis spectrophotometer, measurements were registered in 200–800 nm, using a 1-cm quartz cuvette.

2.3.5. In vitro drug release kinetics

The kinetics of MTX release was determined by UV–Vis spectroscopy at 304 nm. Briefly, 10 mg of nanoparticles were dispersed in 1 mL of phosphate-buffered saline (PBS), pH 5.3 and 7.4, respectively, and placed in a dialysis bag (14,000 Da MWCO). The closed bag was placed in a tube with 10 mL of PBS as the release medium (pH 5.3 and pH 7.4). The tube was maintained under slow stirring at 37 °C. Aliquots of 500 μL were collected at different time points (1, 2, 3, 24, 48, 72 and 96 h) and the volume was replaced with fresh PBS for further correction. The drug release was quantified by UV–Vis.

2.3.6. Cell culture

The RAW 264.7 murine macrophage cell line was cultured in sterile RPMI 1640 medium (Sigma-Aldrich, USA), supplemented with antibiotics (100 μg/mL streptomycin and 100 U/mL penicillin) and 10% foetal bovine serum. The cells were incubated at 37 °C in an incubator with humidified air (85% humidity) and 5% CO_2.

2.3.7. In vitro cellular uptake and CD44 determination

Nanoparticle uptake by macrophage cells was evaluated. Cells were cultured in RPMI 1640 medium and seeded in 48-well tissue culture plates (100,000 cells/well). After 24 h, the medium was removed, and the cells were incubated with 200 μL of each treatment (^{177}Lu-DOTA-HA-PLGA, ^{177}Lu-DOTA-PLGA(MTX) and ^{177}Lu-DOTA-HA-PLGA(MTX)) for 3 h at 37 °C before washing them twice with phosphate-buffered saline (PBS). Then, cells were incubated twice with 500 μL of glycine buffer (50 mM, pH 2.8) for 5 min before collecting the solution in test tubes for measurement (this treatment recovers the nanoparticles bound to the cell membrane; solutions from both washes were

combined). Cells were then incubated twice with 500 μL of 1 M NaOH (1 M) for 5 min, and the solution was collected in test tubes for measurement (this treatment recovers the nanoparticles internalized within the cell; solutions from both washes were combined). Blocking studies were carried out in parallel. The cells were pre-incubated with a concentration 500 times greater than added in the treatment with hyaluronic acid (HA; 0.1 g/mL) for 10 min before addition of the treatments. Radioactivity was measured in samples collected from cells treated with radiolabelled nanoparticles using a NaI(Tl) well detector (NML Inc. USA). The initial activity of each treatment was considered 100%.

CD 44 receptors were identified by immunostaining, briefly, the RAW 264.7 murine macrophage cell were incubated with antibody (anti-CD44) (GENTEX), posteriorly were washed and incubated with secondary antibody Goat Anti- IgG Polyclonal Ab (Dy Light 488, Thermo Fisher Scientific). Cells were washed and mounted in a coverslip previously prepared and observed under fluorescence microscopy, alternative blocking treatment (1% gelatine) was used to distinguishing specific from non-specific staining.

2.3.8. Cell viability assay

Cell viability was assessed in RAW 264.7 cells by using the XTT (2,3-bis
[2-Methoxy-4-nitro-5-sulfophenyl]-2H-tetrazolium-5-carboxyanilide
inner salt; 0.1 mg/mL) assay kit (Roche, Germany). Briefly, RAW 264.7 cells were seeded in 96-well culture plates (10,000 cells/well) and incubated for 24 h. Afterwards, the cells were incubated with 200 μL of each treatment (MTX, PLGA(MTX), HA-PLGA, HA-PLGA(MTX), $^{177}LuCl_3$, ^{177}Lu-DOTA-PLGA(MTX), ^{177}Lu-DOTA-HA-PLGA and ^{177}Lu-DOTA-HA-PLGA(MTX). Treatments with ^{177}Lu had approximately 3 kBq/well, and those with MTX had 48.5 ng. The viability was evaluated at 24, 48 and 120 h after treatment exposure. The cell proliferation percentage in each well was evaluated by the spectrophotometric measurement of cell viability at 450 nm in a microplate absorbance reader (EpochTM, BioTek Instruments, USA). Sample results were evaluated via ANOVA and Bonferroni post hoc tests. The absorbance from untreated cells was considered as 100% viability.

2.4. Statistical analysis

Data was analyzed using OriginPro 8.6 software. Statistical analysis was performed using an univariated ANOVA test followed by the Bonferroni mean comparison (α: 0.05).

3. Results and discussion

The current treatment for RA is focused on achieving the highest level of anti-inflammatory activity, while minimizing joint damage. Due to their variety in physicochemical properties, nanoparticles have been investigated as carriers and drug delivery systems, where macrophages could be considered as a specific target due to its central role in inflammatory disease. Active targeting offers suitable advantages with regard to passive targeting by the enhancement of nanoparticle uptake and optimization of sustained drug delivery [10].

3.1. Chemical characterization

3.1.1. Size of nanoparticles

PLGA nanoparticles were synthetized via the oil-in-water (o/w) emulsification-solvent evaporation method. In the first step, the PLGA polymer was dispersed in organic phase. This mixture was added to an aqueous solution containing a stabilizing agent with posterior evaporation of the solvent in order to induce polymer precipitation as nanoparticles. Table 1 shows the size behaviour during nanoparticle loading and conjugation. The MTX was incorporated into the mixture through the organic solvent phase in order to increase surface area

Table 1
Characteristic distribution parameters in nanoparticulate system mean diameter, SD, PDI and Z potential.

Sample	Diameter (nm) ± SD	PDI	Z potential (mV)
PLGA	152.9 ± 53.3	0.19	- 19.0
PLGA(MTX)	166.1 ± 46.3	0.15	- 21.9
HA-PLGA	161.4 ± 20.1	0.19	- 22.2
HA-PLGA(MTX)	167.6 ± 57.4	0.32	- 18.6

contact with PLGA, maximizing the entrapment efficiency. The PVA solution was used as stabilizer, obtaining a well-dispersed and stable nanoparticle emulsion. Characterization by DLS showed that addition of MTX did not have a significant influence over the hydrodynamic diameter of nanoparticles; mono-modal distribution remained after drug loading (Fig. 2a). Nanoparticle functionalization with hyaluronic acid has been described in medical applications, in order to yield cell binding in joint tissue. The HA was crosslinked to PLGA nanoparticle surface via the carbodiimide reaction. The changes in physicochemical properties are an evidence of adequate surface modifications, because changes in zeta potential have been described when nanoparticles are conjugated to biomolecules [24]. As was observed in PLGA(MTX) nanoparticles, the MTX entrapped in the nanoparticle matrix had no influence over hydrodynamic size with regard to HA-PLGA nanoparticles.

SEM images demonstrated adequate dispersion of polymeric nanoparticles, with spheroidal shapes that correlated with DLS measurements. Fig. 2b shows an example of PLGA nanoparticle distribution found in the analysis. The functionalization with chelating agent DOTA had no effect over size distribution, shape and/or the aggregation state of DOTA-HA-PLGA nanoparticles (Fig. 2c), stoichiometric analysis showed a proportion of 0.16 nmol of DOTA (9.6×10^{16} molecules) per mg of nanoparticles.

The synovium forms a double barrier between plasma and synovial fluid. In rheumatoid arthritis, the increased and discontinuous angiogenesis induces modifications in permeability, which enables passive macromolecular accumulation, whilst interstitial changes restrict synovial permeability to smaller molecules. The proposed nanoparticulate system would allow the permanence of modified nanoparticles in the joint cavity, primarily due to the molecular weight and size (< 200 nm). Horisawa et al. evaluated the size dependency of the D,L-lactide-glycolide copolymer (PLGA) particulates for an intraarticular delivery system through phagocytosis in the rat synovium after directly administering it into the joint cavity. Results showed that fluoresceinamine-bound PLGA (FA-PLGA) microspheres (26.5 μm), administered into the joint cavity, were surrounded by macrophages in the synovium, whereas the FA-PLGA nanospheres (265 nm) were rapidly phagocytosed by the macrophages and transferred into the underlying tissue of the synovium and transferred toward the submembraneous adipose tissue through the cell junction, due to their ability to penetrate the synovium [14].

Senda et al. suggested that synovial cells possess the ability to phagocytose latex particles with sizes close to 240 nm [30], whereas Howie et al. reported that the response of macrophages to particles larger than 5 μm in diameter was approximately the upper limit for biological phagocytosis [15]. Additionally, particle targeting via covalent modifications over the particle surface with the HA corona influences the interaction between surfaces of inflammatory cells, stimulating specific and selective uptake. Additionally, nanoparticles are internalized through CD44-mediated endocytosis processes including pinocytosis, phagocytosis or endocytosis and transported, with eventual formation of lysosomes and consequent delivery of methotrexate in a target-specific manner.

3.1.2. FT-IR

The PLGA nanoparticle spectrum (Supplemental Fig. 1) shows the

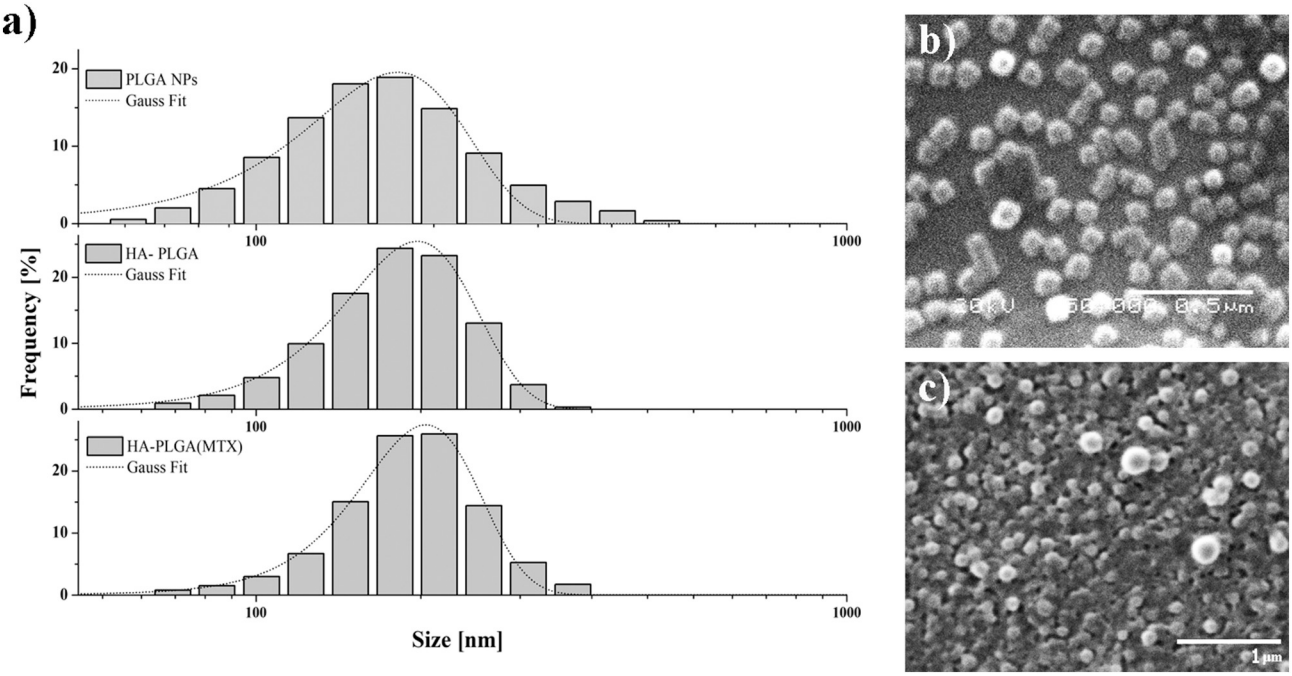

Fig. 2. Size distribution of nanoparticulate systems: a) (PLGA NPs, HA-PLGA and HA-PLGA(MTX)); SEM images of b) PLGA nanoparticles and c) DOTA-HA-PLGA nanoparticles.

same characteristic bands from the polymeric matrix and stabilized core of PLGA previously reported by Stevanović et al. [35]. The PLGA-loaded nanoparticles showed evidence of methotrexate entrapment. The intense band centred at 3272 cm^{-1} provides evidence of the contribution of (O—H)υ and (N—H)υ groups from PLGA nanoparticles and the MTX primary amine, respectively. The bands found at 2916 and 2846 cm^{-1} are attributed to the (C—H)υ; these bands correspond to the interactions between the skeletal carbon of PLGA and MTX. The vibration corresponding to (C = O)υ of carbonyl at 1722 cm^{-1} was shifted to a higher energy, suggesting a strong interaction between MTX and the polymeric nanoparticle matrix. Additional characteristic bands were observed, including the 1422 cm^{-1} mode corresponding to (C—N)υ, 1366 cm^{-1} (C—C)υ, (C—O)υ and (O—H)δ from MTX, and 1240 cm^{-1} assigned to (C—H)δ. Finally, bands at 1087 and 1049 cm^{-1}, corresponding to (C—O)υ, are also observed (Supplemental Fig. 1).

The surface modification of PLGA nanoparticles with HA using a carbodiimide reaction was confirmed by the presence of characteristic bands, suggesting the formation of an amide bound, which is absent in PLGA nanoparticles. Raw material spectra (Supplemental Fig. 2) were consistent with previously-reported analysis [2]. The HA-PLGA nanoparticle spectrum showed characteristic bands. However, a significant increase in intensity was observed at 3286 cm^{-1}, corresponding to the overlapping between the (N—H)υ vibration of the hyaluronic acid molecule and the (O—H)υ of PLGA nanoparticles. Additionally, a positive contribution due to an increase in H-bonding from surface folding, is possible. A well-differentiated band at 2923 cm^{-1}, from aliphatic chains (C—H)υ, was observed. At 1729 and 1638 cm^{-1}, characteristic bands from the (C = O)υ of the ester group were observed, with contribution from the (C—N)υ of amide I. These bands suggest the formation of a covalent bond between PLGA and HA. At 1422 cm^{-1}, the band corresponding to (N—H)δ and (C—N)υ of amide III are seen, as well as the band at 1366 cm^{-1}, corresponding to (C—C)υ, (C—O)υ and (C—H)δ, with a C═O in agreement with previously reported [2,7,35]. Finally, bands at 1240, 1085, 1023 and 835 cm^{-1}, are found, corresponding to (C—H)δ. Vibrations are also present in the spectrum. Moreover, characteristic vibrational modes, specifically from HA, were found at 1561 cm^{-1}, corresponding to (N—H)δ and (C—N)υ in the amide II region found in the hyaluronic acid. In agreement with the evidence observed, we suggest that the surface modification of PLGA nanoparticle with HA results from a complex interaction driven principally by covalent, H-bounding and hydrophilic interactions.

The spectrum of HA-PLGA(MTX) nanoparticles (Fig. 3) shows similar characteristics to that of HA-PLGA nanoparticles. This is because of the overlapping of several bands, which makes the identification of MTX frequencies from other vibrations difficult. Also, the steric impedance decreases the degrees of freedom of the MTX that is encapsulated in the polymer matrix so that its vibrations are very difficult to detect.

The HA-PLGA(MTX) nanoparticle spectrum shows an intense and wide band at 3340 cm^{-1}, corresponding to the overlapping between the (N—H)υ vibration of HA and the (O—H)υ of PLGA nanoparticles. At 2973, 2874 and 2706 cm^{-1}, the bands are due to the (C—H)υ groups. A significant decrease in intensity was probably due to interactions between hydrophilic forces on the nanoparticle surface, allowing the favourable thermodynamic orientation of polymer side groups, whereas the polymer chain backbone and hydrophobic groups are oriented to the nanoparticle core. The band at 1637 cm^{-1} corresponds to (C = O)υ of the ester in PLGA nanoparticles, with contribution from the (C—N)υ of amide I. This band confirms the PLGA conjugation with HA. The band at 1562 cm^{-1} corresponds to the (N—H)δ and (C—N)υ of amide II, present in the hyaluronic acid, and confirms the surface modification of PLGA nanoparticles. The bands at 1481, 1379 and 1255 cm^{-1} correspond to (N—H)δ, (C—O)υ and (C—C)υ vibrations from amide III, respectively. Lastly, bands at 1184, 1045 and 1005 cm^{-1} are related with (C—H)δ and (C—O)υ, present in MTX, PLGA nanoparticles and HA, as previously described by Park et al. [27].

The DOTA-HA-PLGA(MTX) nanoparticle spectrum shows a band at 3350 cm^{-1}, corresponding to (N—H)υ and (O—H)υ; at 2996 and 2949 cm^{-1}, corresponding to (C—H)υ; at 1753 cm^{-1}, corresponding to (C = O)υ; at 1643 cm^{-1}, corresponding to (C = O)υ and amide I (C—N)υ; at 1560 cm^{-1}, corresponding to (N—H)δ and amide II (C—N)υ; at 1425 cm^{-1}, corresponding to (N—H)δ, (C—O)υ and amide III (C—C)υ; at 1388 cm^{-1}, corresponding to (C—O)υ and (N—H)δ; at 1169, 1090 and 1043 cm^{-1}, corresponding to (C—H)δ and (C—O)υ vibrations. Finally, bands near 944 and 750 cm^{-1} confirm the presence of (C—S)υ corresponding to the cysteine present in the chelating agent DOTA,

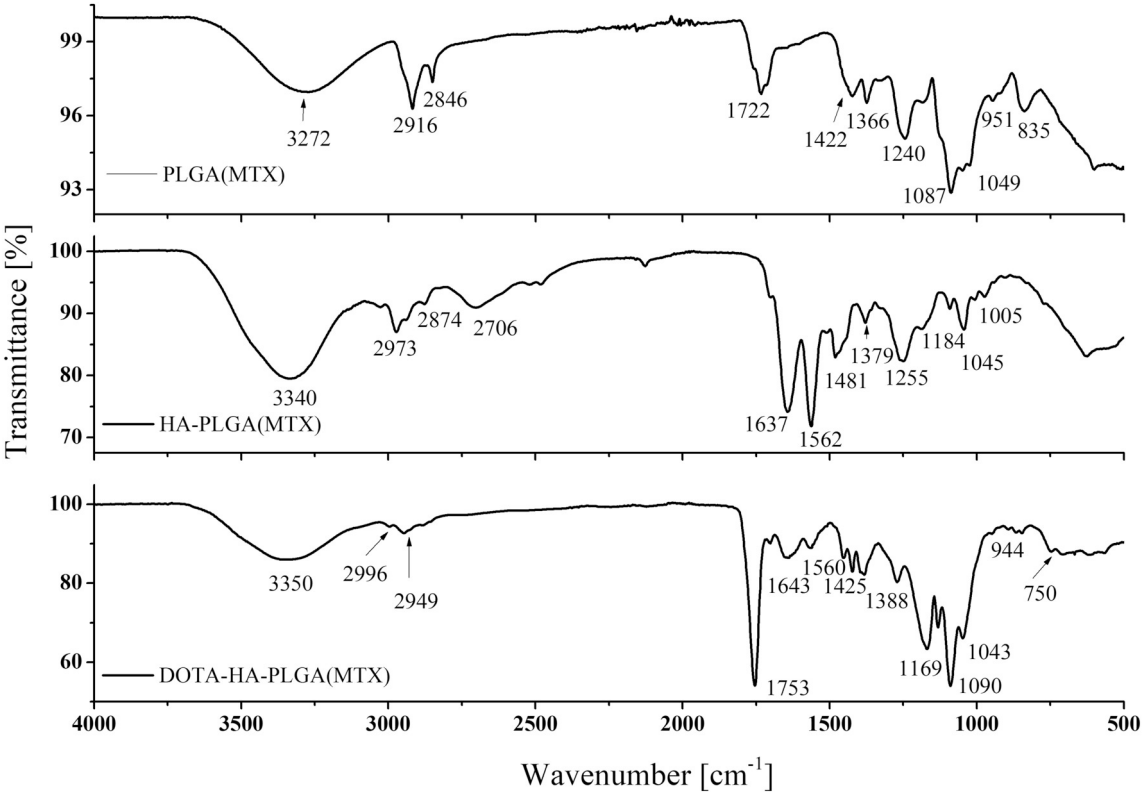

Fig. 3. FT-IR spectra of a) PLGA(MTX) nanoparticles, b) HA-PLGA(MTX) nanoparticles and c) DOTA-HA-PLGA(MTX) nanoparticles.

consistent with the studies of Luna-Gutierrez et al. [22].

Polymer clusters from nanoparticles are arranged in a regular chain of repeating units, where absorption band frequencies depend on the nature of surface irregularities produced by the assembly array. The observed spectra may be interpreted as the result of superposition of vibrational modes from different chemical and conformational entities, as well as steric interactions on nanoparticle cores and surfaces.

3.1.3. UV–Vis

The MTX entrapment was followed spectrophotometrically by UV–Vis. Fig. 4a showed evidence of MTX loading. First, the PLGA nanoparticle spectrum shows a characteristic increase in absorbance in the UV region, with a particular band near 250–280 nm, similar to that reported by Vangara et al. [37]. The MTX spectrum indicates strong transitions in the UV region with bands well-defined at 258 nm, 304 nm and 351 nm, as in the case of Ayyappan [4]. The PLGA(MTX) nanoparticles generated a complex spectrum, with apparent additivity from PLGA and MTX in a certain region. A well-defined band with significant increase in intensity was observed near 260 nm, which is a result of the overlapping between $n \rightarrow \pi^*$ transitions from common carbonyl groups of PLGA and MTX. Specific evidence of MTX entrapment was observed through the presence of a characteristic band near 304 nm, which demonstrated that MTX was loaded.

The HA conjugation to PLGA nanoparticles was also demonstrated (Fig. 4b). The HA spectrum shows a well-defined band at 252 nm, corresponding to carbonyl groups of the HA molecule. When HA is conjugated, the resulting HA-PLGA NP spectrum presents a bathochromic shift to 270 nm, due to the exchange of the oxygen atom and the nitrogen atom of ethylene diamine (EDA), generating a new amide bond. The chelating agent DOTA was also attached to the nanoparticle surface by the HATU reaction. The DOTA molecule showed a spectrum with a characteristic band attributed to carbonyl groups near 250 nm, similar to that reported by Aranda-Lara et al. [3]. Functionalization of HA-PLGA nanoparticles with DOTA showed a complex spectrum with the presence of similar bands identified in the HA-PLGA and DOTA spectrums, demonstrating adequate functionalization.

3.2. Methotrexate (MTX) loading in PLGA nanoparticles

The phenomenon of adsorption in PLGA nanoparticles showed a linear increase of the entrapped drug in the polymeric matrix as a function of the increase in the amount of methotrexate, methotrexate accessibility during nanoparticle formation improves the load with respect to preformed nuclei for the loading of drugs. Maximum entrapment efficiency (EE) was found near 95%, with a corresponding loading efficiency (LE) of 6% (see Fig. 5). The amount of entrapped MTX was also determined directly by measuring the MTX inside the nanoparticles, the EE was found superior to 60% however, for a direct method nanoparticles must be dissolved in an organic solvent and posteriorly re-dispersed in a proper medium, complete isolation and redissolving are affected by surfactants and polymer fragments which interfere in the quantification of MTX. We conclude that indirect method for MTX determination was superior to direct method.

Regarding the amount of MTX entrapped in nanoparticle matrix, it was observed that associated drug to the polymeric matrix of nanoparticles is the result of physicochemical properties of the interacting materials, as well as the specific surface area of PLGA nanoparticles and affinity between MTX and the polymeric matrix. Increases on polymer concentration during nanoparticle preparation would result in significant increase of LE, however nanoparticles size and kinetic parameters must be monitored.

3.3. ^{177}Lu radiolabelling

The radiochemical purity of the multifunctional ^{177}Lu-DOTA-HA-PLGA(MTX) nanoparticle was 96 ± 2%, determined by ITLC. Radiolabelling of HA-PLGA modified nanoparticles was carried out using the chelating agent DOTA, which has been used for peptide,

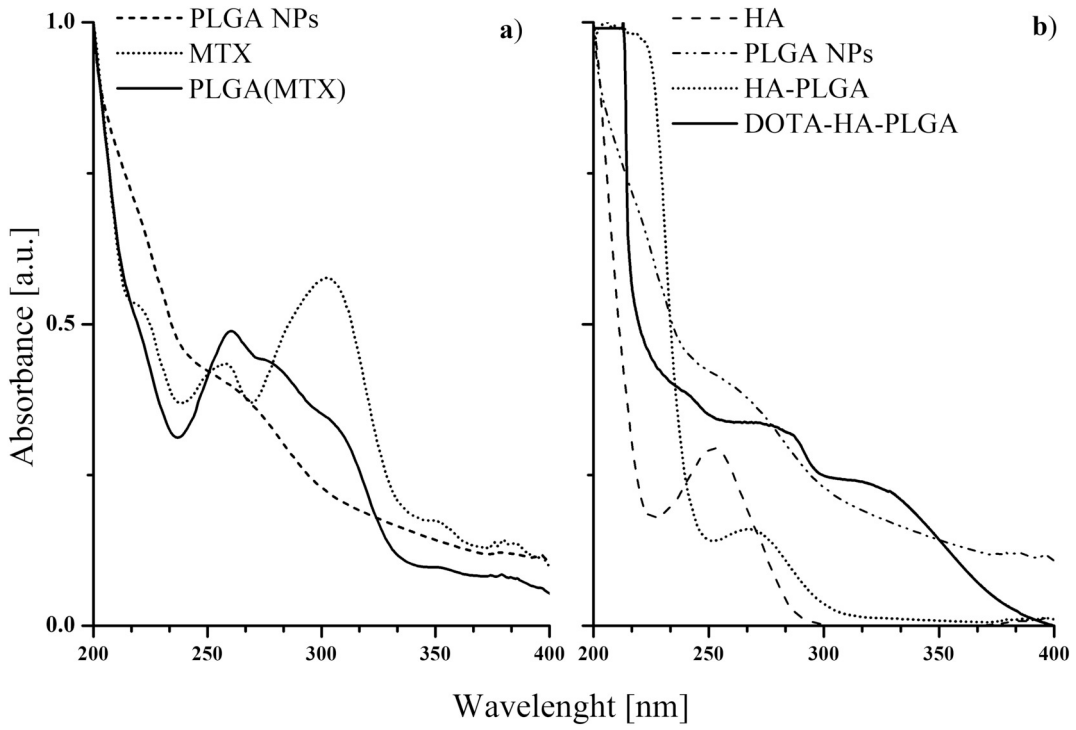

Fig. 4. UV–Vis spectra of a) PLGA nanoparticles, MTX and PLGA(MTX) nanoparticles; b) HA, PLGA nanoparticles, HA-PLGA nanoparticles and DOTA-HA-PLGA nanoparticles.

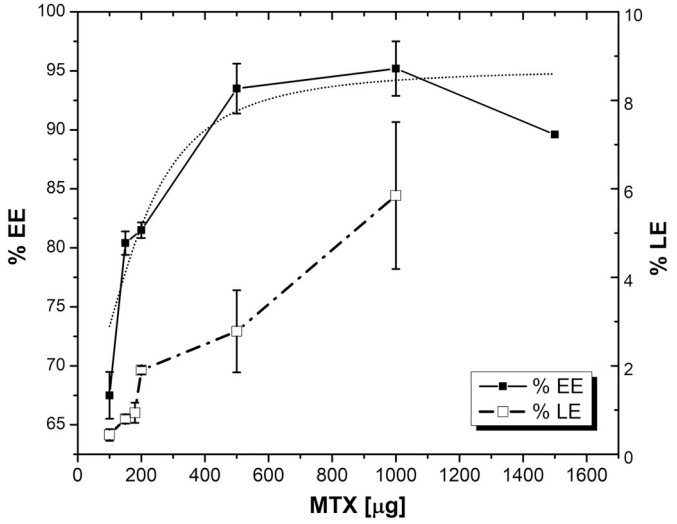

Fig. 5. Entrapment and loading efficiency of methotrexate (MTX) in PLGA nanoparticles.

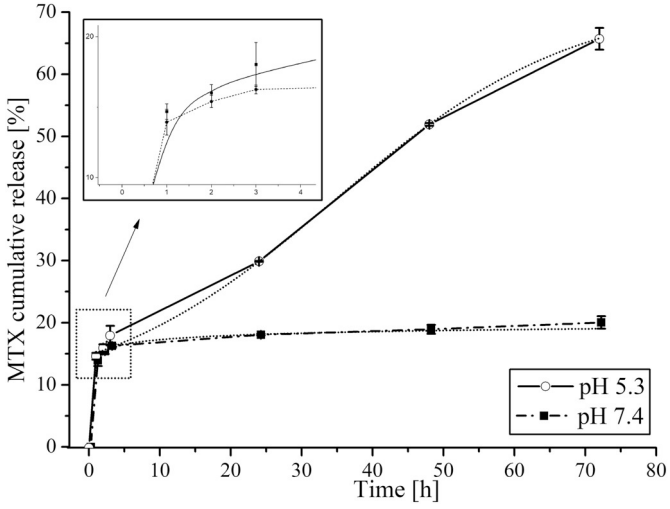

Fig. 6. In vitro release profile of HA-PLGA(MTX) nanoparticles at pH 5.3 and 7.4.

antibodies, steroids and small molecule radiolabelling, with high thermodynamic stability and kinetic inertness, also suitable for use as a therapeutic radionuclide for targeting purposes [5,6]. Chelating anchorage to the nanoparticle surface and posterior radiolabelling does not have significant influence over the hydrodynamic radio. The molecular weight of chelating agents was negligible regarding nanoparticle size.

3.4. In vitro drug release profile

To evaluate the potential of HA-PLGA(MTX) nanoparticles as a drug carrier, the in vitro release of MTX at two different pH values (7.4 and 5.3), was evaluated. Fig. 6 shows that the polymeric nanoparticles preserve their drug content at physiologic pH, with a maximum release of MTX near 25% of the loaded drug. The profile is characterized by a bi-phasic response. The initial and fast phase ("burst") reaches at least 16% of the drug- releasing capacity after 3 h. The slow phase continues with the release of < 5% of the total drug content in the posterior 70 h. Evidences suggests that the mechanism is driven by MTX diffusion through filled pores from HA and consequent diffusion through the polymer matrix (HA-PLGA), corresponding with bi-phasic behaviour. When nanoparticles are exposed to an acidic pH, an increase in the accumulative amount of the released drug was observed, suggesting a significant modification in the releasing mechanisms; during the first 3 h, there are no significant changes in the releasing profile corresponding to physiologic pH. Thereafter, the mechanism could be driven by a combination between a diffusion process and the surface erosion of the HA corona, resulting in the consequent bulk erosion of the

polymeric matrix, reaching a release of 70% at 80 h, however elucidation of drug release mechanism is out of our goal. A mathematical model (growth/sigmoidal) predicts that 100% of drug is achieved close to 100 h. In vivo tests are required to evaluate the influence of the chemical and biological environment on the nanoparticle payload.

3.5. In vitro cellular uptake study

Macrophages, abundant in the inflamed synovial membrane, possess broad pro-inflammatory potential and contribute considerably to inflammation and joint destruction. Due to their successful response to anti-rheumatic therapy, selective delivery of nanomedicine to active macrophages by binding to a specific receptor could switch off their complex connections with other cells to ameliorate the RA condition while maintaining the biological functions of the resting macrophages [9].

It is known that the interactions between HA and CD44 are subject to tight regulations such that the receptor is normally maintained in a quiescent state, showing little appreciable HA binding. For example, although freshly-isolated peripheral blood monocytes and lymphocytes express CD44, they do not bind to HA. During inflammation, however, the pro-inflammatory cytokine tumour necrosis factor R (TNF-R) induces sulfurylation and subsequent conformational changes of CD44, which transforms it into a form with much greater HA affinity [18].

To demonstrate the specific uptake of ^{177}Lu-DOTA-HA-PLGA, ^{177}Lu-DOTA-HA-PLGA(MTX) and ^{177}Lu-DOTA-PLGA(MTX) nanoparticles via the HA receptor, uptake and internalization assays in cells were carried out. For therapeutic intervention, specific binding to inflammatory cells and subsequent internalization is one of the most critical steps in order to obtain a desirable effect. The cell-surface receptor CD44 in macrophages is a potentially-rewarding target in joint disease. Fig. 7a shows the results for the uptake assay on RAW 264.7 cells. Passive uptake (non-specific uptake) was determined using the ^{177}Lu-DOTA-PLGA(MTX) treatment (without HA). A significant difference, with an eight-fold increase in nanoparticle uptake, was observed when hyaluronic acid was present (^{177}Lu-DOTA-HA-PLGA and ^{177}Lu-DOTA-HA-PLGA(MTX)). The amount of methotrexate in nanoparticles does not affect CD44 recognition. When cells were previously treated with HA in order to block CD44 receptors, the uptake decreased significantly with regard to the group of unblocked receptors (~40%). It is known that extracellular HA is typically endocytosed into lysosomes [18] and the internalization assay (Fig. 7b) showed a linear and positive correlation with regard to nanoparticle uptake. At least 10% of associated activity was found in cytosolic compartment. The internalization behaviour in blocked cells was similar to that of unblocked cells, demonstrating that passive uptake was carried out by a surface phenomenon between nanoparticles and the cell surface, whereas internalization is driven by CD44-mediated uptake with consequent internalization and intracellular metabolism. These results prove that the presence of HA on the nanoparticle surface was crucial for uptake and the specific recognition of the nanosystem ^{177}Lu-HA-PLGA(MTX) for CD44 receptors. Immunohistochemical staining showed the specific binding of the antibodies to CD44 cell receptors on RAW 264.7 cell line (Fig. 7c), in agreement with studies reported previously [13,25].

3.6. Cell viability assay

The effect of the treatment with $^{177}LuCl_3$, ^{177}Lu-DOTA-HA-PLGA, ^{177}Lu-DOTA-PLGA(MTX) and ^{177}Lu-DOTA-HA-PLGA(MTX) nanoparticles, as well as MTX, HA-PLGA, PLGA(MTX) and HA-PLGA(MTX) nanoparticles (Fig. 8) was evaluated in RAW 264.7 cells and analyzed by the ANOVA test, followed by the Bonferroni test for media

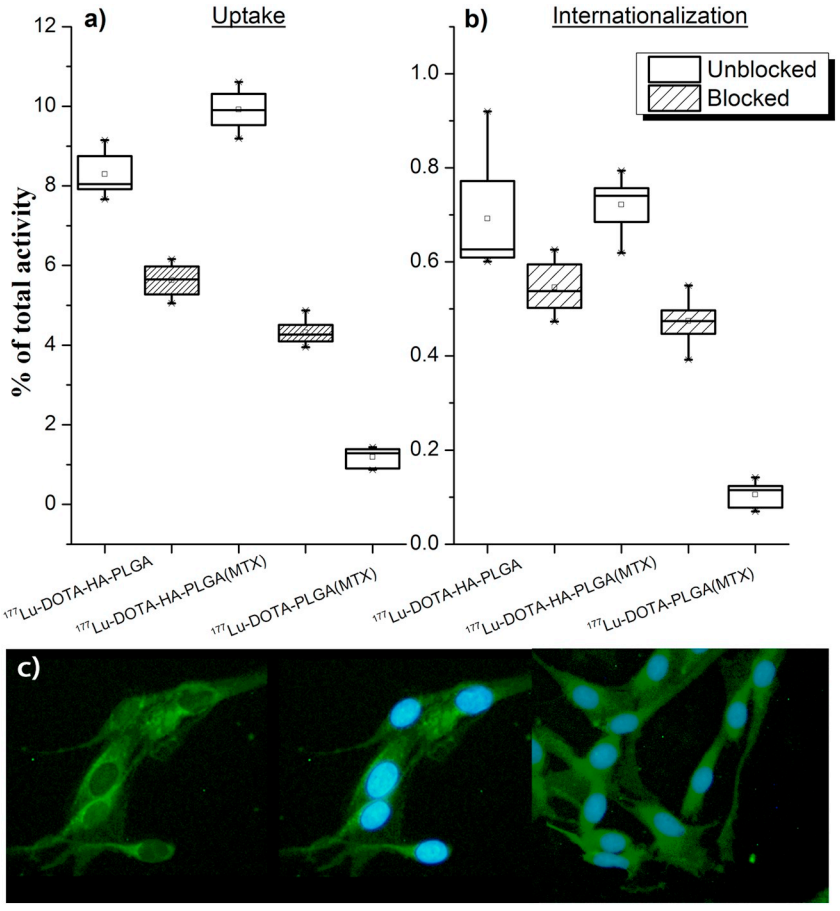

Fig. 7. Cellular uptake (a) and internalization (b) of ^{177}Lu-DOTA-HA-PLGA, ^{177}Lu-DOTA-HA-PLGA(MTX) and ^{177}Lu-DOTA-PLGA(MTX) nanoparticles by blocked HA-receptor RAW 264.7 cells and non-blocked receptor RAW 264.7 cells. (c) Immunohistochemistry staining of CD44 receptor on RAW 264.7 cells, blue: nuclei, green: primary antibody. (For interpretation of the references to colour in this figure legend, the reader is referred to the web version of this article.)

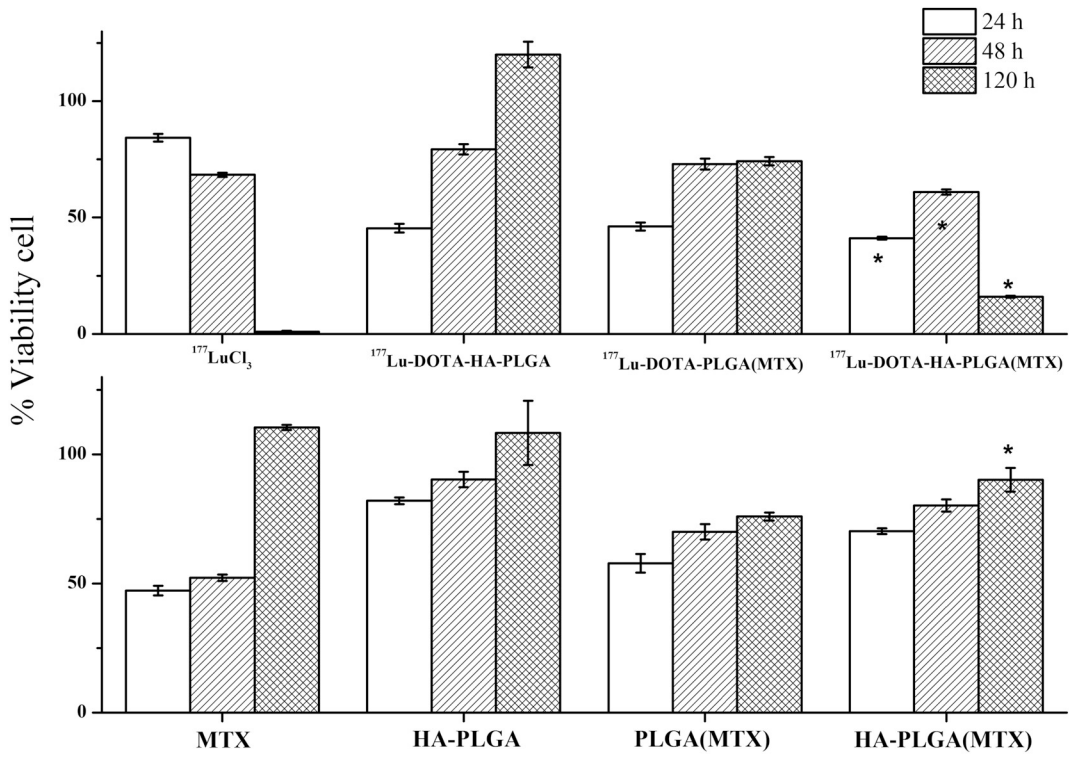

Fig. 8. Cell viability of RAW 264.7 cells after exposure to ^{177}LuCl3, ^{177}Lu-DOTA-HA-PLGA, ^{177}Lu-DOTA-PLGA(MTX), ^{177}Lu-DOTA-HA-PLGA(MTX), (MTX), HA-PLGA, PLGA(MTX) and HA-PLGA(MTX) at 24 h, 48 h and 120 h.

comparison (significance level set at $p \leq 0.05$).

The response to MTX was characterized by a reduction of 50% in cell viability, with a recovery in proliferation phase after 48 h. Methotrexate is characterized by cellular uptake mediated by folate carrier FC receptors. When cells were exposed to free MTX, cell proliferation showed a significant inhibition of 50% at 24 and 48 h, whereas PLGA(MTX) and HA-PLGA(MTX) reached a maximum cytotoxic effect of 42% and 32% at 24 h, respectively, and 31% and 20% at 48 h, respectively. The differences in cell survival could be explained as follows: the free MTX generated a "bolus" exposure, increasing the availability in a short period of time. However, in agreement with the release profile, at 48 h only a concentration close to 50% of entrapped MTX has been released. This means that local concentration of free MTX was less, but with a constant rate of appearance from the nanoparticulate systems. Consequently, the time of exposure to the free drug increases according to the rate phenomena of release driven by *endo*-lysosomal activity. Previous studies in which MTX was injected into the joint in single small doses failed to produce clinical efficacy and have been explained by the rapid clearance of MTX from the knee joint and insufficient exposure of proliferating cells in the joint to the drug [8].

Gao et al. [12] demonstrate that entrapped drugs in polymeric micelles was more effective than free drug (Docetaxel), with an enhancement in cytotoxicity, more sustained in vitro release behaviour, slower extravasation from blood vessels in animal model and a significant concentration increase in target tissues [12]. The cells exposed to HA-PLGA showed a maintenance in cell viability, it has been widely demonstrated that polymers have a good biocompatibility, biodegradability and nonimmunogenicity. HA is one of the most abundant mammalian polysaccharides, found in the body, such as extracellular matrix and synovial fluid, whereas PLGA has been successfully used as a biodegradable polymer, because it undergoes hydrolysis in the body to produce the original monomer, lactic acid and glycolic acid, both intermediaries in oxidative metabolisms [16,17,28].

In the HA-PLGA(MTX) group, the response at 120 h was superior to 75% in cell viability. Increases in cell viability have been reported in nanoparticulate drug delivery systems based on hyaluronic acid, due to the fact that HA is the main component of the extracellular matrix and can provide cell adherence, with consequent stimulation over cell culture proliferation [23,39].

The group exposed to $^{177}LuCl_3$ showed a characteristic response to radiation exposure, with an exponential decrease in cell viability, reaching 95% in cell inhibition at around 120 h of exposure. It is important to note that, due to the physical behaviour at 120 h, only 40% of radiation decay was achieved. The increase in cell damage by radiation could be explained by the increase of oxidative stress produced by radiolysis in the surrounding media and inside the cell.

The group exposed to ^{177}Lu-DOTA-HA-PLGA(MTX) was significantly inhibited compared to ^{177}Lu-DOTA-PLGA(MTX) and PLGA(MTX) ($p < 0.05$), which was attributed to the increase in cell uptake and internalization as a result of the presence of HA.

The present study develops a multifunctional system based on polymeric PLGA nanoparticles conjugated to hyaluronic acid for methotrexate delivery, a drug used as the gold standard in RA treatment. Additionally, the system was conjugated to the DOTA chelating agent and posteriorly radiolabelled with ^{177}Lu, for radiosynovectomy.

Actually, beta-emitters have a mean energy and range in tissue from 0.34 MeV with 0.33 mm of range (^{169}Er) to 2.27 MeV and 3.6 mm of range (90Y). ^{90}Y is administrated as citrate or colloidal silicate, especially in knee, and ^{186}Re has been used in hip, shoulder, ankle, elbow and wrist [36].

Recently, ^{177}Lu has emerged as a pivotal radionuclide, due to its suitable nuclear decay characteristics. It has many advantages when compared to other therapeutic radionuclides (^{198}Au, ^{90}Y, ^{32}P, ^{186}Re, ^{169}Er, etc.), for the potential treatment of RA, such as the emission of $\beta-$ particles, their energies and abundance ($t_{1/2}$ = 6.71 d, E_β [max] = 497 keV, $E\gamma$ = 113 keV [6.4%], 208 keV [11%] and 0.7 mm range in tissue) [32]. Radiocolloidal formulations for sinoviortesis increase uptake at the surface of the synovial tissue. The additional advantage of the colloidal state is targeting the CD44 receptor with HA to increase the therapeutic effect through the antiproliferative response.

Shinto et al. reported that the intra-articular injection of ^{177}Lu-HA (dose of 333 ± 46 MBq) in the knee produced pain relief and improved mobility in all patients treated [32].

In order to assess its therapeutic potential, ^{177}Lu-DOTA-HA-PLGA(MTX) nanoparticles need to be tested on in vivo models to elucidate the physiological kinetics as well as dosimetric evaluation of radiolabelled nanoparticles in normal and abnormal synovial tissue.

4. Conclusion

Herein, we have reported the proper preparation of a multifunctional chemo/radiotherapy agent based on a polymeric nanoparticulate system, spectroscopic characterization demonstrates the adequate surface modification by HA and successful conjugation to DOTA as a chelating agent for Lutetium-177. The in vitro release kinetics and in vitro cytotoxicity assays on RAW 264.7 cells demonstrated an enhancement in nanoparticle uptake and the cytotoxic effect mediated by HA binding and consequent internalization. These results suggest that ^{177}Lu-DOTA-HA-PLGA(MTX) is a potential drug carrier for further specific targeted applications in anti-rheumatic therapy.

Acknowledgements

This study was supported by the “Universidad Autónoma del Estado de México” (Project No. 4288/2017/CI), the International Atomic Energy Agency (CRP—F22064, Contract No. 18358) and the Mexican National Council (grant SEP-CONACYT A1-S-38087). It was performed as part of the activities of the “Laboratorio Nacional de Investigación y Desarrollo de Radiofármacos, LANIDER- CONACyT”.

Appendix A. Supplementary data

Supplementary data to this article can be found online at https://doi.org/10.1016/j.msec.2019.109766.

References

[1] Samira Sadat Abolmaali, Ali Mohammad Tamaddon, Rassoul Dinarvand, A review of therapeutic challenges and achievements of methotrexate delivery systems for treatment of cancer and rheumatoid arthritis, Cancer Chemother. Pharmacol. 71 (5) (2013) 1115–1130, https://doi.org/10.1007/s00280-012-2062-0.

[2] Yahya Mrestani Alkrad, et al., Characterization of enzymatically digested hyaluronic acid using NMR, Raman, IR, and UV–vis spectroscopies, J. Pharm. Biomed. Anal. 31 (3) (2003) 545–550, https://doi.org/10.1016/S0731-7085(02)00682-9.

[3] Liliana Aranda-Lara, Guillermina Ferro-Flores, Erika Azorín-Vega, Flor de María Ramírez, Nallely Jiménez-Mancilla, Blanca Ocampo-García, Clara Santos-Cuevas, Keila Isaac-Olivé, Synthesis and evaluation of Lys 1 (α,γ-folate)Lys 3 (^{177}Lu-DOTA)-Bombesin(1-14) as a potential theranostic radiopharmaceutical for breast cancer, Appl. Radiat. Isot. 107 (January) (2016) 214–219, https://doi.org/10.1016/j.apradiso.2015.10.030.

[4] S. Ayyappan, N. Sundaraganesan, V. Aroulmoji, E. Murano, S. Sebastian, Molecular structure, vibrational spectra and DFT molecular orbital calculations (TD-DFT and NMR) of the antiproliferative drug methotrexate, Spectrochim. Acta A Mol. Biomol. Spectrosc. 77 (1) (2010) 264–275, https://doi.org/10.1016/j.saa.2010.05.021.

[5] S. Banerjee, S.O. Raja, M. Sardar, N. Gayathri, B. Ghosh, a. Dasgupta, Iron oxide nanoparticles coated with gold: enhanced magnetic moment due to interfacial effects, J. Appl. Phys. 109 (12) (2011) 1–8, https://doi.org/10.1063/1.3596760.

[6] Sharmila Banerjee, M.R.A. Pillai, F.F. (Russ) Knapp, Lutetium-177 therapeutic radiopharmaceuticals: linking chemistry, radiochemistry, and practical applications, Chem. Rev. 115 (8) (2015) 2934–2974, https://doi.org/10.1021/cr500171e.

[7] Andreas Barth, Infrared spectroscopy of proteins, Biochimica et Biophysica Acta (BBA) - Bioenergetics 1767 (9) (2007) 1073–1101, https://doi.org/10.1016/j.bbabio.2007.06.004.

[8] Helen M. Burt, Antonia Tsallas, Samuel Gilchrist, Linda S. Liang, Intra-articular drug delivery systems: overcoming the shortcomings of joint disease therapy, Expert Opinion on Drug Delivery 6 (1) (2009) 17–26, https://doi.org/10.1517/17425240802647259.

[9] Minglei Chen, Kambere Amerigos Daddy J.C, Yanyu Xiao, Qineng Ping, Li Zong, Advanced nanomedicine for rheumatoid arthritis treatment: focus on active targeting, Expert Opinion on Drug Delivery 14 (10) (2017) 1141–1144, https://doi.org/10.1080/17425247.2017.1372746.

[10] Sanam Dolati, Sanam Sadreddini, Davoud Rostamzadeh, Majid Ahmadi, Utilization of Nanoparticle Technology in Rheumatoid Arthritis Treatment, vol. 80, (2016), pp. 30–41 ScienceDirect.

[11] Guillermina Ferro-Flores, Blanca E. Ocampo-García, Clara L. Santos-Cuevas, Flor de María Ramírez, Erika P. Azorín-Vega, Laura Meléndez-Alafort, Theranostic radiopharmaceuticals based on gold nanoparticles labeled with (177)Lu and conjugated to peptides, Curr. Radiopharm. 8 (2) (2015) 150–159 http://www.ncbi.nlm.nih.gov/pubmed/25771363.

[12] Gao Xiang, Shimin Wang, BiLan Wang, Senyi Deng, Xiaoxiao Liu, XiaoNing Zhang, LinLi Luo, et al., Improving the anti-ovarian cancer activity of docetaxel with biodegradable self-assembly micelles through various evaluations, Biomaterials 53 (June) (2015) 646–658, https://doi.org/10.1016/j.biomaterials.2015.02.108.

[13] Yifat Glucksam-Galnoy, Tsaffrir Zor, Rimona Margalit, Hyaluronan-modified and regular multilamellar liposomes provide sub-cellular targeting to macrophages, without eliciting a pro-inflammatory response, J. Control. Release 160 (2) (2012) 388–393, https://doi.org/10.1016/j.jconrel.2011.10.008.

[14] Eijiro Horisawa, Katsuaki Kubota, Izumi Tuboi, Keiichi Sato, Hiromitsu Yamamoto, Hirofumi Takeuchi, Yoshiaki Kawashima, Size-dependency of DL-lactide/glycolide copolymer particulates for intra-articular delivery system on phagocytosis in rat synovium, Pharm. Res. 19 (2) (2002) 132–139 http://www.ncbi.nlm.nih.gov/pubmed/11883639.

[15] D.W. Howie, B. Manthey, S. Hay, B. Vernon-Roberts, The synovial response to intraarticular injection in rats of polyethylene Wear particles, Clinical Orthopaedics and Related Research 292 (July) (1993) 352–357.

[16] Gangliang Huang, Hualiang Huang, Application of hyaluronic acid as carriers in drug delivery, Drug Delivery 25 (1) (2018) 766–772, https://doi.org/10.1080/10717544.2018.1450910.

[17] Laura Jaimes-Aguirre, Enrique Morales-Avila, B.E. Blanca E. Ocampo-García, L.A. Luis Alberto Medina, Gustavo López-Téllez, B.V. Brenda V. Gibbens-Bandala, Vanessa Izquierdo-Sánchez, Biodegradable poly(D,L-lactide-co-glycolide)/poly(L-γ-glutamic acid) nanoparticles conjugated to folic acid for targeted delivery of doxorubicin, Mater. Sci. Eng. C 76 (July) (2017) 743–751, https://doi.org/10.1016/j.msec.2017.03.145.

[18] Kamat Medha, Kheireddine El-boubbou, David C. Zhu, Teri Lansdell, Xiaowei Lu, Wei Li, Hyaluronic Acid Immobilized Magnetic Nanoparticles for Active Targeting and Imaging of Macrophages, (2010), pp. 2128–2135.

[19] Zulfequar Ahamad Khan, Rahul Tripathi, Brahmeshwar Mishra, Methotrexate: a detailed review on drug delivery and clinical aspects, Expert Opinion on Drug Delivery 9 (2) (2012) 151–169, https://doi.org/10.1517/17425247.2012.642362.

[20] Linda S. Liang, Paul T. Salo, David A. Hart, Helen M. Burt, Intra-articular treatment of inflammatory arthritis with microsphere formulations of methotrexate: pharmacokinetics and efficacy determination in antigen-induced arthritic rabbits, Inflamm. Res. 58 (8) (2009) 445–456, https://doi.org/10.1007/s00011-009-0009-7.

[21] Haiyue Long, Xiaoling Li, Zitai Sang, Lan Mei, Tao Yang, Zicheng Li, Liangxue Zhou, et al., Improving the pharmacokinetics and tissue distribution of pyrinezolid by self-assembled polymeric micelles, Colloids Surf. B: Biointerfaces 156 (August) (2017) 149–156, https://doi.org/10.1016/j.colsurfb.2017.05.014.

[22] Myrna Luna-Gutiérrez, Guillermina Ferro-Flores, Blanca E. Ocampo-García, Clara L. Santos-Cuevas, Nallely Jiménez-Mancilla, L.M. De León-Rodríguez, Erika Azorín-Vega, Keila Isaac-Olivé, A therapeutic system of ^{177}Lu-labeled gold nanoparticles-RGD internalized in breast cancer cells, J. Mex. Chem. Soc. 57 (3) (2013) 212–219.

[23] Fadee G. Mondalek, Richard A. Ashley, Christopher C. Roth, Yusuf Kibar, Nabeel Shakir, Michael A. Ihnat, Kar-Ming Fung, Brian P. Grady, Bradley P. Kropp, Hsueh-kung Lin, Enhanced angiogenesis of modified porcine small intestinal submucosa with hyaluronic acid-poly(lactide-co-glycolide) nanoparticles: from fabrication to preclinical validation, J. Biomed. Mater. Res. A (2010), https://doi.org/10.1002/jbm.a.32748 9999A: NA-NA.

[24] Marco P. Monopoli, Christoffer Åberg, Anna Salvati, Kenneth A. Dawson, Biomolecular coronas provide the biological identity of nanosized materials, Nat. Nanotechnol. 7 (12) (2012) 779–786, https://doi.org/10.1038/nnano.2012.207.

[25] Tobias Nyström, Ponuts Dunér, Anna Hultgårdh-Nilsson, A constitutive endogenous osteopontin production is important for macrophage function and differentiation, Exp. Cell Res. 313 (6) (2007) 1149–1160, https://doi.org/10.1016/j.yexcr.2006.12.026.

[26] Shweta Pandey, Asiya Mahtab, Nishant Rai, Purnima Rawat, Farhan J.F.J. Ahmad, Sushama Talegaonkar, Emerging role of CD44 receptor as a potential target in disease diagnosis: a patent review, Recent Patents Inflamm. Allergy Drug Discov. 11 (2) (2017) 77–91, https://doi.org/10.2174/1872213X11666170907111858.

[27] Si-Nae Park, Jong-Chul Park, Hea Ok Kim, Min Jung Song, Hwal Suh, Characterization of porous collagen/hyaluronic acid scaffold modified by 1-ethyl-3-(3-dimethylaminopropyl)carbodiimide cross-linking, Biomaterials 23 (4) (2002) 1205–1212, https://doi.org/10.1016/S0142-9612(01)00235-6.

[28] N. Vijayakameswara Rao, Hong Yeol Yoon, Hwa Seung Han, Hyewon Ko, Soyoung Son, Minchang Lee, Hansang Lee, Dong-Gyu Jo, Young Mo Kang, Jae Hyung Park, Recent developments in hyaluronic acid-based nanomedicine for targeted cancer treatment, Expert Opinion on Drug Delivery 13 (2) (2016) 239–252, https://doi.org/10.1517/17425247.2016.1112374.

[29] Linda T. Senbanjo, Meenakshi A. Chellaiah, CD44: a multifunctional cell surface adhesion receptor is a regulator of progression and metastasis of cancer cells, Frontiers in Cell and Developmental Biology 5 (March) (2017), https://doi.org/10.3389/fcell.2017.00018.

[30] H. Senda, E. Sakuma, I. Wada, H.J. Wang, H. Maruyama, N. Matsui, Ultrastructural study of cells at the synovium-cartilage junction: response of synovial cells of the rat knee joint to intra-articularly injected latex particles, Kaibogaku Zasshi. Journal of Anatomy 74 (5) (1999) 525–535.

[31] Jung Min Shin, Seol-Hee Kim, Thavasyappan Thambi, Dong Gil You, Jueun Jeon, Jong Oh. Lee, Bong Youl Chung, Dong-Gyu Jo, Jae Hyung Park, A hyaluronic acid–methotrexate conjugate for targeted therapy of rheumatoid arthritis, Chem.

Commun. 50 (57) (2014) 7632, https://doi.org/10.1039/c4cc02595d.
[32] Ajit S. Shinto, K.K. Kamaleshwaran, Sudipta Chakraborty, K. Vyshakh, S.G. Thirumalaisamy, S. Karthik, V.N. Nagaprabhu, K.V. Vimalnath, Tapas Das, Sharmila Banerjee, Radiosynovectomy of painful synovitis of knee joints due to rheumatoid arthritis by intra-articular administration of Lu-labeled hydroxyapatite particulates: first human study and initial Indian experience, World Journal of Nuclear Medicine 14 (2) (2015), https://doi.org/10.4103/1450-1147.153908.
[33] Jeffrey A. Sparks, Medha Barbhaiya, Elizabeth W. Karlson, Susan Y. Ritter, Soumya Raychaudhuri, Cassandra C. Corrigan, Fengxin Lu, et al., Investigating methotrexate toxicity within a randomized double-blinded, placebo-controlled trial: rationale and design of the Cardiovascular Inflammation Reduction Trial-Adverse Events (CIRT-AE) study, Semin. Arthritis Rheum. 47 (1) (2017) 133–142, https://doi.org/10.1016/j.semarthrit.2017.02.003.
[34] Magdalena M. Stevanovi, Branka Jordovi, Preparation and Characterization of Poly (D,L-Lactide-Co-Glycolide) Nanoparticles Containing Ascorbic Acid, vol. 2007, (2007), https://doi.org/10.1155/2007/84965.
[35] Magdalena M. Stevanović, Branka Jordović, Dragan P. Uskoković, Preparation and characterization of poly(D,L-lactide-co-glycolide) nanoparticles containing ascorbic acid, J. Biomed. Biotechnol. 2007 (2007), https://doi.org/10.1155/2007/84965.
[36] B.M.B. Torres, P.F.E. Ayra, R.E. Garcia, D.N. Cornejo, H. Yoriyaz, Perfiles de Dosis Absorbida vs Profundidad de Tejido Sinovial Para El Y-90 y El P-32 Empleados En Tratamiento de Radiosinoviortesis, American Congress of the IRPA, Mexico (2006) 1–11 http://www.iaea.org/inis/collection/NCLCollectionStore/_Public/38/030/38030456.pdf?r=1.
[37] Kiran Kumar Vangara, Jingbo Louise Liu, Srinath Palakurthi, Hyaluronic acid-decorated PLGA-PEG nanoparticles for targeted delivery of SN-38 to ovarian cancer, Anticancer Res. 33 (6) (2013) 2425–2434 http://www.ncbi.nlm.nih.gov/pubmed/23749891.
[38] A. Vilchis-Juárez, G. Ferro-Flores, C. Santos-Cuevas, E. Morales-Avila, B. Ocampo-García, L. Díaz-Nieto, M. Luna-Gutiérrez, N. Jiménez-Mancilla, M. Pedraza-López, L. Gómez-Oliván, Molecular targeting radiotherapy with cyclo-RGDfK(C) peptides conjugated to ^{177}Lu-labeled gold nanoparticles in tumor-bearing mice, J. Biomed. Nanotechnol. 10 (3) (2014), https://doi.org/10.1166/jbn.2014.1721.
[39] Ying Wang, Yue Teng Wei, Zhao Hui Zu, Rong Kai Ju, Mu Yao Guo, Xiu Mei Wang, Qun Yuan Xu, Fu Zhai Cui, Combination of hyaluronic acid hydrogel scaffold and PLGA microspheres for supporting survival of neural stem cells, Pharm. Res. 28 (6) (2011) 1406–1414, https://doi.org/10.1007/s11095-011-0452-3.
[40] Joanna Zalewska, Małgorzata Węgierska, Tacjana Barczyńska, Marzena Waszczak, Paweł Żuchowski, Sławomir Jeka, Efficacy of radiation synovectomy (radiosynovectomy or radiosynoviorthesis) with yttrium-90 in exudative inflammation of synovial membrane of knee joints in patients with rheumatic diseases – preliminary report, Reumatologia/Rheumatology 1 (2016) 3–9, https://doi.org/10.5114/reum.2016.58754.